Ezrin Mutants Affecting Dimerization and Activation†

David N. Chambers‡ and Anthony Bretscher*

Department of Molecular Biology and Genetics, Biotechnology Building, Cornell University, Ithaca, New York 14853

Received September 10, 2004; Revised Manuscript Received November 23, 2004

ABSTRACT: ERM (ezrin/radixin/moesin) proteins provide a regulated linkage between membrane-associated proteins and the actin cytoskeleton. Previous work has shown that ezrin can exist in a dormant monomeric state in which the N-terminal FERM domain is tightly associated with the C-ERMAD (carboxyl-terminal ERM association domain), masking binding sites for at least some ligands, including F-actin and the scaffolding protein EBP50. Activation of ezrin requires relief of the intramolecular association, and this is believed to involve phosphorylation of threonine 567. Studies have therefore employed the T567D phosphomimetic mutant to explore the consequences of ezrin activation in vivo. Ezrin also exists as a stable dimer, in which the orientation of the two subunits is unknown, but might involve the central α-helical region predicted to form a coiled−coil. By characterization of ezrin mutants, we show that relief of the intramolecular association in the monomer results in unmasking of ligand binding sites and a significant conformational change, that the T567D mutation has a small effect on the biochemical activation of ezrin, and that the predicted coiled−coil region does not drive dimer formation. These results provide strong support for the conformational activation model of ezrin, elucidate the basis for dimer formation, and reveal that a mutant generally considered to be fully activated is not.

Ezrin is the founding member of a conserved family, the ezrin/radixin/moesin (ERM)[1] proteins, that provides a regulated linkage in cell surface structures between cortical microfilaments and the plasma membrane (reviewed in refs *1*−*3*). Cells in which ERM expression has been knocked down lose surface microvilli, thereby implicating these proteins in microvillus formation or stabilization (*4*).

ERM proteins have an N-terminal FERM domain of ∼300 amino acid residues, followed by a region of ∼170 residues predicted to be α-helical with a high potential to form a coiled−coil, and then terminate in a ∼100 residue domain (*5*−*7*). Since the C-terminal domain of any ERM member can bind to the FERM domain of any ERM protein, this region has been called the C-ERMAD (C-terminal ERM association domain) (*8*). The dormant form of ezrin in which the FERM domain is associated with the C-ERMAD is unable to bind at least some ligands. Thus, whereas the isolated FERM domain can bind to the scaffolding proteins EBP50 and E3KARP, and the regulator RhoGDI, these binding sites are masked when the C-ERMAD is bound (*9*, *10*). The FERM domain can also bind a number of other membrane associated proteins, including CD43; CD44; CD95; ICAM-1, -2, -3; and NHE-1 (*11*−*16*), but in these cases it is not yet clear whether the binding sites are masked by C-ERMAD binding. To provide a linkage to actin, an F-actin binding site is located in the C-terminal 30 residues of the C-ERMAD, and this site is also masked in the dormant protein (*8*, *17*−*19*). Since binding sites are masked in the dormant protein, a working model was developed in which activation involves relief of the FERM/C-ERMAD interaction to unmask these sites (*8*), a model that is also consistent with in vivo studies involving expression of ezrin domains (*20*, *21*). Recent structural evidence also supports this model. The atomic structure of the moesin FERM/C-ERMAD complex reveals a tri-lobed FERM domain to which an extended C-ERMAD binds (*22*). EBP50 binds to the same surface on the FERM domain as the last helix of the C-ERMAD, thereby explaining why EBP50 does not bind to the dormant ezrin molecule (*23*). Moreover, structural analysis of the isolated FERM domains of ezrin, radixin, and moesin suggest a significant structural change upon C-ERMAD binding that could also indirectly change the affinity or availability of the FERM domain for other ligands (*24*−*26*).

Given the apparent need to activate ERM proteins by hindering the FERM/C-ERMAD interaction, considerable work has been devoted to investigating how this might be achieved. The first evidence for regulation was the finding that phosphorylation of threonine 558 in the C-ERMAD of moesin increases upon platelet activation (*27*). Phosphorylation of this residue reduces the FERM/C-ERMAD interaction without affecting the C-terminal F-actin binding activity (*28*). Subsequently, it was shown that in vitro unmasking of both F-actin and EBP50 binding sites in dormant ezrin or moesin requires both participation of a lipid, which can be PIP_2, and phosphorylation of the appropriate threonine (558 in moesin, 567 in ezrin) (*29*, *30*). Recent evidence suggests that lipid binding is a prerequisite for threonine phosphorylation in ERM activation (*31*). Given this background, a

† This work was supported by PHS Grant GM36652.

* Corresponding author. Tel.: (607) 255-5713. Fax: (607) 255-6249. E-mail: apb5@cornell.edu.

‡ Present address: Department of Natural Sciences, Science Building, Northeastern State University, Tahlequah, OK 74464.

[1] Abbreviations: EBP50, ERM binding phosphoprotein of 50 kDa; E3KARP, exchanger 3 kinase A regulatory protein; ERM, ezrin, radixin, moesin; C-ERMAD, carboxyl-terminal ERM association domain; FERM, four point one, ERM.

10.1021/bi0480382 CCC: $30.25
Published on Web 02/08/2005

number of laboratories have used a phosphomimetic mutant of ezrin in which threonine 567 was mutated to aspartic acid (T567D) to explore the function of activated ezrin. Indeed, cells transfected to express a C-terminal tagged version of this mutant appear to induce microvilli in vivo (*32*, *33*). Despite these in vivo phenomena, the biochemical properties of the ezrin T567D mutant have not yet been compared with wild-type ezrin.

Although largely monomeric, another intriguing feature of ERM proteins is their ability to form homo- and heterodimers (*34*). Ezrin dimer formation was found to be enhanced in cultured A431 cells following stimulation with epidermal growth factor, and dimers were highly enriched in extracts of isolated placental microvilli (*35*). Ezrin monomers and dimers in placental tissue are sufficiently stable so they can be separated and purified (*36*). Both the biological function of dimers (*33*, *35*) and their molecular arrangement is unresolved. It has been suggested that dimers might be composed of antiparallel subunits held together by two FERM/C-ERMAD associations (*36*). An alternative possibility is a parallel association in which the central α-helical region assembles a coiled−coil to drive dimer formation yielding a molecule with two FERM domains on one end and two C-ERMADs on the other for linking from membrane proteins to the cytoskeleton (*37*).

In this paper, we compare the biochemical properties of wild-type ezrin with two site-directed mutants, studies that shed light on the molecular organization of ezrin dimers, the conformation of activated ezrin, and the degree of activation of the T567D mutant.

EXPERIMENTAL PROCEDURES

Ezrin Expression Constructs. Plasmids for the bacterial expression of wild-type untagged ezrin (pQE16-ezrin) and Ez1-584 (pQE16-Ez-1-584) have been described (*9*). To generate a plasmid for EzT567D expression, the T567D mutation was generated by PCR from pQE16-ezrin using the Stratagene QuickChange Site Directed Mutagenesis Kit (#200518, La Jolla, CA) and the primers 5′-CAAGGCCGGGACAAGTACAAGGACCTGCGGCAGATC-3′ and 5′-GCCCTGCCGGATCTGCCGCAGGTCCTTGTACTTGTC-3′. The plasmid was then digested using Dra III and Hind III to isolate the mutated C-ERMAD. The resulting fragment was ligated into the similarly digested original pQE16-ezrin plasmid, and the resulting clones were verified by DNA sequencing. The pQE16-Ez-T567D plasmid was transformed into *Escherichia coli* strain BL21 containing pREP4 repressor plasmid for expression.

Expression and Purification of Recombinant Proteins. Expression and purification of wild-type, Ez1-584, EzT567D, and FERM domain ezrin constructs was performed as described (*9*). Briefly, a 1 L bacterial culture was grown at 37 °C to an A_{600} of 0.9 and induced with 2 mM IPTG for 3 h. Cells were pelleted at 7000*g*, 4 °C for 20 min, and then resuspended in 20 mL of 10 mM Tris-HCl pH 7.4 and 150 mM NaCl, and repelleted at 40 000*g*, 4 °C for 15 min. The pellet was then resuspended in 35 mL of HA buffer A (160 mM K_2HPO_4 −KH_2PO_4, pH 7.0) containing 50 μg/mL PMSF and 75 μg/mL benzamidine, sonicated to lyse bacteria, and centrifuged at 40 000*g*, 4 °C for 20 min to produce a clarified bacterial extract. The supernatant was loaded into a 50 mL FPLC superloop and applied to a hydroxyapatite (HA-Ultragel, Pharmacia) column (8 cm long with radius of 0.5 cm), washed with 60 mL of HA buffer, and eluted using a 120 mL gradient from 160 to 800 mM phosphate. The 1.5 mL fractions were collected and analyzed by SDS−PAGE. Fractions rich in ezrin were pooled, giving a total volume of between 15 and 30 mL, depending on purification. Pooled fractions were dialyzed into buffer A (20 mM MES, 150 mM NaCl, pH 6.7) utilizing three 1 L buffer changes for a minimum of 2 h in each and then clarified by centrifugation at 40 000*g*, 4 °C for 20 min. The supernatant was loaded onto an *S*-Sepharose column (6 cm long with a radius of 0.5) equilibrated with buffer A. The column was washed with 60 mL of buffer A and eluted using an 80 mL 150 mM to 1 M NaCl gradient. The 1 mL fractions were collected and analyzed by SDS−PAGE. The resulting fractions were pooled or used individually.

Western Blotting. Western blotting was performed by running 10% SDS−PAGE gels and transferring them to polyvinylidene fluoride membranes (Immobilon-P, Millipore, Bedford, MA) with a semi-dry transfer system (Integrated Separation Systems, Hyde Park, MA). Briefly, the SDS−PAGE mini-gels were run at a constant current of 24 mA until the dye front reached the base of the gel, usually about 1 h. Proteins in the gel were transferred to the membrane at 1.5 mA/cm^2 *x* (surface area of gel) for 90 min. To verify transfer and identify molecular weight markers, the membrane was stained with Ponceau S. The membrane was then blocked overnight in wash buffer (50 mM Tris, 150 mM NaCl, 1% Tween 20, pH 8.3) plus 10% w/v fatfree dry milk, incubated with primary antibody for 1 h, and incubated for 30 min in secondary antibody. After blocking and each antibody incubation, the membrane was washed vigorously 3 times for 5 min on a rocker with wash buffer. Blots were developed using enhanced chemiluminescence (ECL, Amersham; Arlington Heights, IL) and recorded on Kodak diagnostic film (Rochester, NY). Primary antibody was mouse anti-ezrin tail (Zymed Labs Inc.) (1:1000) or rabbit ezrin antiserum (1:10 000). Secondary antibodies were HRP conjugated goat anti-mouse (Invitrogen, Carlsbad, CA) (1:5000) and HRP conjugated goat anti-rabbit (ICN, Costa Mesa, CA) (1:10 000).

Sucrose Gradient Sedimentation. Sedimentation was performed using 11 × 60 mm tubes (#5010, Seton Scientific, Sunnyvale, CA) with 5−20% w/v sucrose gradients in 20 mM HEPES, 1 mM DTT, pH 7.4 at two different NaCl concentrations, 150 and 500 mM, which gave similar results. A total of 100 μL of 2 mg/mL wild-type or 1-584 was loaded on the top of the sucrose gradient and centrifuged in a Beckman SW60 rotor at 44 000*g* for 16 h at 4 °C; all samples were run in duplicate. A 20 gauge needle was inserted into the bottom of each tube, and 200 μL fractions were collected and analyzed by 10% SDS−PAGE. Sedimentation coefficients were estimated by comparison with the following standards run in parallel: bovine erythrocyte aldolase (7.35 *S*), bovine serum albumin (4.35 *S*), and carbonic anhydrase (3.2 *S*). Sedimentation coefficients from four tubes from two separate runs were averaged for each protein.

Gel Filtration. Gel filtration was performed on a Superose 6 HR 10/30 (Pharmacia) column using 20 mM HEPES, 1 mM DTT, pH 7.4 at two different NaCl concentrations, 150 and 500 mM NaCl, with similar results. A total of 200 μL

of 2 mg/mL protein solution was loaded on the column, which was eluted at 0.2 mL/min, and 500 μL fractions were collected. The fractions were analyzed by 10% SDS−PAGE and subsequent Coomassie Brilliant Blue staining. Gels were scanned to determine the amount of each protein species in each fraction. The Stokes radii were estimated by comparison with the following standards run in the same set of runs: carbonic anhydrase (24 Å), bovine serum albumin (36 Å), equine apoferritin (67 Å), and bovine thyroglobulin (85 Å). Three separate runs for each protein analyzed were averaged to determine the Stokes radius of each sample.

Immobilization of the Ezrin FERM Domain, GST-C-ERMAD, and GST-EBP50 (320−358). The FERM domain covalently immobilized on beads was prepared from recombinant free FERM domain, containing ezrin residues 1−297 as described (*38*).

Beads with immobilized recombinant GST-EBP50 (320−358), which contains the binding site for the ezrin FERM domain, and recombinant GST-C-ERMAD (480−586) were prepared as described (*9*).

Ligand Binding Assays. The 50 μL of bead slurry (12.5 μL of beads) was mixed with proteins in 50 mM Tris, 150 mM NaCl, pH 7.4 plus 1% Triton X-100 for 30 min to a 500 μL final volume at 4 °C and maintained in suspension by being rolled on a rotating drum. Beads were sedimented by quick spins to 14 000 rpm in an Eppendorf microfuge. The supernatants were removed, and beads washed 5 times by being vortexed for 30 s in 1.25 mL of the same buffer followed by sedimentation and removal of supernatant. Bound proteins were eluted from the beads with 100 μL of Laemmli buffer (*39*), boiled for 5 min, and analyzed by SDS−PAGE.

Quantitation. Quantitation of SDS−PAGE bands was performed using Imagequant software (Amersham Pharmacia, Piscataway, NJ) with the local background correction setting. Values were imported into Microsoft Excel, where graphs were generated.

RESULTS

Design, Expression, and Purification of Wild-Type and Mutant Ezrin Proteins. Earlier work has shown that ezrin purified from human placenta, the richest known tissue source of ezrin, exists as a mixture of globular monomers and elongated dimers. Remarkably, the monomers and dimers are sufficiently stable to interconversion that they can be purified separately (*36*). Neither monomer nor dimer can bind F-actin or EBP50, suggesting that in both conformations these sites, in the C-ERMAD and FERM domain, respectively, are masked. This suggests that in the dimer, each of the FERM domains is associated with a C-ERMAD. The simplest interpretation is that the dimer consists of two antiparallel subunits with associated FERM/C-ERMADs (*36*). However, the central α-helical region is strongly predicted to form a coiled−coil when analyzed using the Parcoil and Multicoil programs. It is therefore of interest to know if this region contributes to dimer formation. One way to test this is by generating mutations that inhibit the ability of the C-ERMAD to bind the FERM domain and then determine if the mutant protein can form dimers. According to the conformational activation model described previously, such mutants should also be active. Thus, the generation and characterization of such mutants should allow us to examine both the requirements for dimer formation and the properties of activated mutants.

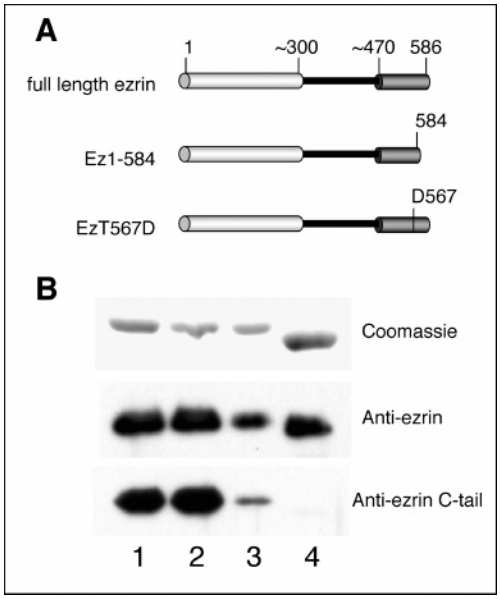

FIGURE 1: Ezrin species used in this study. (A) Schematic diagram of wild-type, Ez1-584, and ET567D constructs. (B) 10% SDS−PAGE analysis of purified proteins. Lane 1, wild-type ezrin; lane 2, EzT567D; lane 3, Ez1-584; and lane 4, Ez1-567. Western blot of the purified proteins probed with B23 ezrin antibody detects all ezrin species. Western blot probed with monoclonal antibody generated to the C-terminal 10 residues of ezrin fails to detect Ez1-567.

The C-terminal two residues of ezrin's C-ERMAD are critical for high affinity binding to the FERM domain (*8*). The first construct made, Ez1-584 (Figure 1A) is therefore predicted to have a defective C-ERMAD. As discussed in the introductory paragraphs, the second mutant, EzT567D (Figure 1A), is also predicted to have a defective C-ERMAD, and its characterization might also reveal information about dimer formation and activation.

To ensure that no complications arose from the use of tagged proteins, wild-type ezrin, Ez1-584, and EzT567D were all expressed in bacteria and purified as untagged proteins for biochemical characterization. Purification involved making bacterial lysates and then fractionating them on a hydroxyapatite column, which previous work had shown affords an extraordinary enrichment step for both the wild-type protein and the isolated FERM domain (*36*, *38*, *40*). When each protein was then subjected to anion exchange chromatography on *S*-Sepharose, purified protein was obtained for further analysis (Figure 1B).

Expression of the Ez1-584 construct yielded two species, a minor one migrating on SDS−PAGE with the same mobility as wild-type ezrin, and a major one with a slightly higher mobility whose relative abundance increased during purification, which we interpret as a proteolytically clipped version of Ez1-584. On the basis of mobility in SDS gels, we estimate that about 2.4 kDa is removed, corresponding to about 20 amino acid residues. MALDI-TOF gave a molecular weight consistent with loss of the 17 additional C-terminal residues, suggesting that it represents Ez1-567. To establish which end of the molecule was trimmed, we analyzed immunoblots using a monoclonal antibody raised

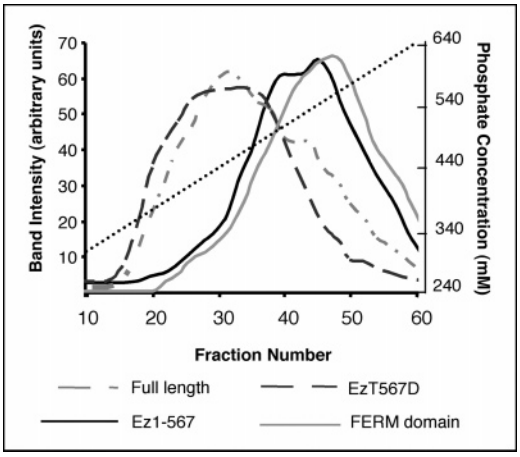

FIGURE 2: Elution profile on the hydroxyapatite column of wild-type ezrin, Ez1-567, EzT567D, and the ezrin FERM domain. Profiles were generated by Coomassie stained SDS gels of each fraction being scanned, followed by optical densitometry.

to the C-terminal 10 residues of ezrin in comparison with a polyclonal antiserum raised against the whole protein (Figure 1B). Fortunately, we were able to purify a small amount of the unclipped Ez1-584 construct that migrated with wild-type ezrin as an internal control in these analyses. While the polyclonal antiserum recognized wild-type ezrin, Ez1-584, the clipped Ez1-584 species, and EzT567D, the monoclonal antibody raised to the C-terminal 10 residues of ezrin recognized wild-type and EzT567D well, but was less efficient at recognizing Ez1-584, and showed no reactivity toward the clipped species. We therefore conclude that the clipped Ez1-584 species has 17 residues removed from its C-terminus and is therefore designated Ez1-567.

Ez1-567 Has an Active FERM Domain. Studies on ezrin have been greatly assisted by the finding that ezrin and its isolated FERM domain bind tightly to hydroxyapatite. During these studies, we noted that a higher concentration of phosphate was needed to elute the isolated FERM domain than the wild-type molecule, which has a FERM/C-ERMAD association (Figure 2). Since the FERM domain seems to be the region of the protein with high affinity for hydroxyapatite, the elution difference suggests that the association of the C-ERMAD in the wild-type protein might reduce its affinity for hydroxyapatite. Thus, the elution position of an ezrin construct may provide an indication of the degree to which the FERM domain is free of an associated C-ERMAD. Analysis of Ez1-567 showed that it eluted at the same phosphate concentration as the isolated FERM domain and is therefore predicted to have a free FERM domain.

The accessibility of ligand binding sites in Ez1-567 was determined by immobilizing known ligands on beads and assessing their ability to retain wild-type ezrin or Ez1-567 (Figure 3). The ligands tested were immobilized FERM domain (lane F) to test for an available C-ERMAD, GST-Ez-C-ERMAD (lane C) to test for an available FERM domain, and GST-EBP50 (lane E) to test for the availability of the EBP50 binding site. While wild-type ezrin showed only trace binding to all of these beads, Ez1-567 bound to GST-C-ERMAD and GST-EBP50 but not the FERM domain. Thus, Ez1-567 has a FERM domain with unmasked binding sites for the C-ERMAD and EBP50, but it has a defective C-ERMAD that is unable to bind the FERM domain.

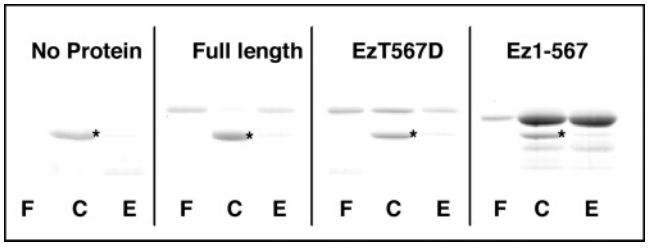

FIGURE 3: Assessment of available ligand binding sites of purified ezrin species. Purified proteins as indicated were incubated with beads to which the ezrin FERM domain (F), or GST-Ez-C-ERMAD (C), or GST-EBP50 (320−358) (E) were immobilized, and the beads were washed and eluted with SDS. Stained gels after analysis of the eluates by SDS−PAGE are shown. The GST-C-ERMAD that elutes from the glutathione beads is indicated (∗).

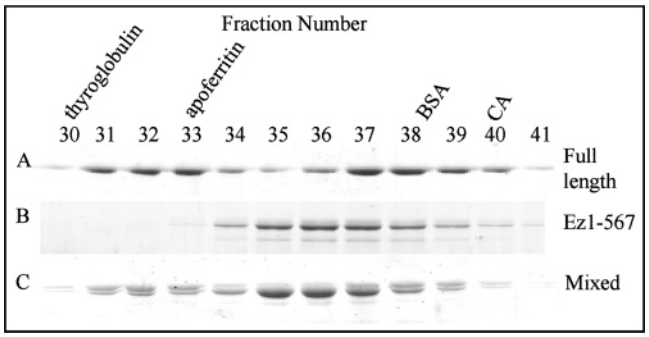

FIGURE 4: Superose 6 HR 10/30 gel filtration analysis of wild-type ezrin (A), Ez1-567 (B), and a mixture of wild-type and Ez1-567 (C). SDS−PAGE of the relevant fractions are shown. The migration position of standards is indicated above the fraction numbers.

Ez1-567 Is an Elongated Monomer. As discussed previously, ezrin purified from human placental tissue exists as relatively stable globular monomers (Stokes radius of 41 Å) and elongated dimers (Stokes radius of 72 Å) (*36*). We first wanted to determine whether this is also true of ezrin expressed in, and purified from, bacteria. Gel filtration analysis of bacterially expressed and purified ezrin on a calibrated Superose 6 column yielded two species with Stokes radii of 41 and 74 Å (Figure 4), indicating that a similar monomer/dimer ezrin mixture is obtained after expression in bacteria. Gel filtration analysis of Ez1-567 revealed that it migrates as a single species with a larger Stokes radius (48 Å) than the purified wild-type monomer (41 Å) (Figure 4B). To evaluate the subunit composition of the Ez1-567 species, we determined its sedimentation coefficient in sucrose gradients to be 3.6*S* (Table 1). From these hydrodynamic data, we calculate (*41*) that Ez1-567 has a molecular weight of about 74 kDa indicating that it is a monomer in solution. Moreover, since it has a larger Stokes radius and smaller sedimentation coefficient than the dormant monomer, it is more extended as reflected in a higher calculated frictional coefficient (Table 1).

Since Ez1-567 has no tendency to form dimers, our results demonstrate that homodimer formation requires an intact ezrin C-terminus. It also tells us that the central α-helical region of ezrin is by itself unable to drive dimer formation, despite its predicted propensity to form a coiled−coil.

To determine whether Ez1-567 is inherently unable to form dimers, we mixed it with an excess of wild-type ezrin and allowed the mixture to sit at 4 °C for 1 day before analyzing it by gel filtration. Because of the faster migration of Ez1-

Table 1: Hydrodynamic Data for Ezrin Species

ezrin species	sequence M_r (Da)	native[a] M_r (Da)	Stokes radius (Å)	sedimentation value (*S*)	frictional coefficient[b] f/f_o
wild-type monomer	69 398	68 000	41 ± 1[c]	3.9 ± 0.1	1.5
wild-type dimmer	138 796	143 000	74 ± 1	4.5 ± 0.1	2.1
Ez1-567	66 984	74 000	48 ± 1	3.6 ± 0.1	1.8
EzT567D monomer	69 412	73 000	43 ± 1	3.9 ± 0.1	1.6

[a] Calculated from the relationship: native molecular weight = 430 × Stokes radius (Å) × sedimentation coefficient (*41*). [b] Calculated from $f/f_o = R_s(4\pi N/3\upsilon M_r)1/3$, where R_s is the experimentally determined Stokes radius, N is Avogadro's number (6.02×10^{23}), υ is the partial specific volume (taken to be 0.74 cm^3/g), and M_r is the sequence molecular mass. [c] Average values are given; all determinations fell within the indicated ranges.

567 on SDS−PAGE, we were able to distinguish it from wild-type ezrin. This analysis (Figure 4C) revealed that Ez1-567 can heterodimerize with wild-type ezrin, presumably through an association between the FERM domain of Ez1−567 and a C-ERMAD of the wild-type protein. These data support a dimer model where formation is driven by the FERM/C-ERMAD interaction. Since the FERM domains are masked in the dimer (*36*), the only simple model for dimers, compatible with the results, is one with two associated FERM/C-ERMADs with the subunits in an antiparallel configuration.

EzT567D Retains a Weakened C-ERMAD. Our second construct EzT567D, believed to have a defective C-ERMAD, was analyzed in a similar manner. Elution from the hydroxyapatite column was similar to wild-type ezrin (Figure 2), suggesting that the FERM domain of EzT567D is not fully accessible. Ligand binding assays, to assess the ability of EzT567D to bind immobilized FERM domain (lane F), immobilized GST-C-ERMAD (lane C), and immobilized GST-EBP50 (lane E), revealed that it is not significantly retained on either FERM or GST-EBP50 resins. It is, however, retained to a small extent on the GST-C-ERMAD beads (Figure 3). This indicates that the higher affinity of the exogeneous wild-type C-ERMAD has the ability to displace the T567D C-ERMAD under the conditions used in these experiments. In addition, since EzT567D is not retained on the GST-EBP50 beads, the affinity of the T567D C-ERMAD for the FERM domain is sufficient to preclude binding to EBP50.

These initially surprising results suggest that a C-ERMAD containing T567D still has a very significant ability to bind the FERM domain. On the basis of our analysis of ezrin dimers described previously, another test of the FERM/C-ERMAD interaction is whether EzT567D can form dimers. Gel filtration analysis indeed revealed that EzT567D can form both globular monomers and elongated dimers having a dimer Stokes radius very similar to wild-type ezrin and a slightly larger monomer Stokes radius (43 Å) (Figure 5A). Dimer stability can be assessed by collecting the dimer fraction, concentrating it, and resolving it on the gel filtration column. When this is done with ezrin dimers isolated either from placenta (*36*), or after bacterial expression (Figure 5B), the majority of the dimer fraction migrates at the position of the dimer. However, when this analysis is performed with the EzT567D dimers, most of them dissociate into monomers (Figure 5C).

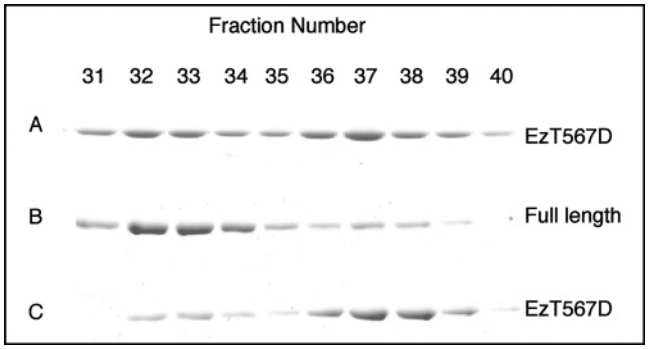

FIGURE 5: Superose 6 HR 10/30 gel filtration analysis of EzT567D (A), dimer peak from wild-type ezrin (B), and the dimer peak from EzT567D (C). SDS−PAGE of the relevant fractions are shown.

Thus, EzT567D has a partially functional C-ERMAD that is sufficiently active to allow the formation of dimers and to mask the EBP50 binding site. The slightly increased Stokes radius of the EzT567D monomer is consistent with the idea that in the equilibrium between closed and open conformations, the EzT567D monomer spends more time in the open state than does wild-type ezrin.

In Vivo Analysis of EzT567D. Since the EzT567D construct appeared to still have masked binding sites on its FERM domain, we explored whether it behaved as an activated molecule upon expression in cultured cells. For expression studies, we generated wild-type ezrin and EzT567D constructs with Xpress tags on their N-terminus. These were expressed in two cells types, the porcine kidney LLC-PK1 cells used by Gautreau and colleagues (*33*), which have abundant apical microvilli, and 3T3 mouse fibroblasts that normally have very few microvilli. We could find no phenotypic differences between expression of wild-type ezrin and T567D in these cells in terms of the number of microvilli, the localization of the expressed protein, and the distribution of actin (data not shown). In work currently in progress, we have generated active ezrin constructs that drive the assembly of massive numbers of microvilli in the 3T3 cell system, so this lack of an effect is not simply a technical problem with these cells.

DISCUSSION

The analysis presented in this study strongly supports the conformational regulation model suggested for ERM proteins (*8*) as well as providing insight into the structure of ezrin dimers and the role of threonine 567 in ezrin regulation.

Dormant ezrin, isolated from tissues (*36*, *42*) or after expression in bacteria (this study), is normally a monomeric protein that is fairly globular as determined by hydrodynamic data. The rotary shadow image for dormant radixin (*43*) is consistent with this view. Activation, resulting from the release of the FERM/C-ERMAD association, is likely to result in a less compact molecule. Indeed, the Ez1-567 species we have analyzed has both unmasked binding sites in the FERM domain as well as a more elongated structure (Table 1), with a calculated frictional coefficient f/f_o of 1.8, as compared with the f/f_o of 1.5 for the dormant wild-type monomer and 2.1 for the elongated wild-type dimer isolated from tissues (*36*) or after bacterial expression (this study).

The finding that Ez1-567 shows no propensity to form dimers demonstrates that the C-terminal 19 residues of the

C-ERMAD are essential for dimer formation and that an intact central α-helical region is insufficient for dimer formation. Recent studies reported after this work was completed (*44*) show that the isolated central domain of radixin is an extended α-helix as predicted but fails to dimerize, consistent with the results reported here. Since this region does not spontaneously dimerize, any coiled−coil formed by the α-helical regions must be guided together by the FERM/C-ERMAD associations.

Antiparallel coiled−coils between associated subunits are rare. The longest antiparallel coiled−coil reported is in bacterial SMC proteins that have 300 residue coiled−coils (*45*). The possible presence in the extended dimer of a ~170 residue antiparallel coiled−coil demands an explanation for the function of the α-helical region in ezrin, which is conserved in predicted properties and length in ERM proteins from nematodes to mammals. It could serve as a binding site for associated molecules, and indeed, the regulatory subunit of protein kinase A has been reported to bind to this region (*46*). Alternatively, the dimers might perform a heretofore unappreciated role in which the FERM/C-ERMADs have to be held rigidly apart.

Our data on the structure of dormant ezrin monomers and dimers are interesting in light of the images of dormant wild-type and mutant radixin (T564A, being the threonine corresponding to T567 in ezrin) and active radixin (T564E) (*43*). Dormant wild-type and T564A radixin exist, like ezrin, as a mixture of monomers and dimers. Low angle rotary shadowing of this mixture revealed only globular structures 8−14 nm in diameter; it was therefore suggested that both monomers and dimers are globular. This contrasts with our results in which monomers have hydrodynamic data consistent with a globular conformation and dimers have hydrodynamic data consistent with a relatively elongated conformation. The active radixin mutant (T564E) imaged by Ishikawa et al. migrated primarily as a monomer on gel filtration and had an extended form, with two globular structures (~5−8 nm) connected by a 20−25 nm filamentous structure, a distance that could accommodate a ~170 residue α-helix. The authors suggest that this represents the FERM domain, the C-ERMAD, and the intervening α-helical region. However, it is possible that it might also represent the antiparallel dimer, as dimers are also present in their preparation.

The finding that the T567D mutation has only a small effect on the FERM/C-ERMAD interaction was initially surprising as this mutation has often been used to explore the in vivo consequences of expressing activated ezrin. However, in studies in which this mutation has been employed, it has generally been used in a construct also containing a C-terminal tag. We have resisted using C-terminal tags as our structural data on the moesin FERM/C-ERMAD complex (*22*) shows that the hydroxyl of the C-terminal carboxylic acid makes a hydrogen bond with asparagine 210 and serine 214 in the moesin FERM domain, and this interaction is likely to contribute significantly to the FERM/C-ERMAD association. Indeed, we had previously found that loss of the last two residues from the C-ERMAD greatly reduces interaction with the FERM domains as assessed by blot overlays (*8*), although solution studies revealed some remaining affinity (*47*). It is therefore likely that in the context of a C-terminal tag in which the hydrogen bonds with asparagine 210 and threonine 214 (serine 214 in moesin) is compromised, T567D might have a much more significant effect on the FERM/C-ERMAD interaction than in the untagged situation. It will therefore be important to generate mutants that are activated in the absence of a C-terminal tag and see what their biochemical properties are and what effects they confer when expressed in various contexts. Such studies are presently underway.

ACKNOWLEDGMENT

We thank Dr. P. Andrew Karplus for his comments on this manuscript.

REFERENCES

1. Bretscher, A., Edwards, K., and Fehon, R. G. (2002) ERM proteins and merlin: integrators at the cell cortex, *Nat. Rev. Cell Mol. Biol. 3*, 586−599.
2. Gautreau, A., Louvard, D., and Arpin, M. (2002) ERM proteins and NF2 tumor suppressor: the Yin and Yang of cortical actin organization and cell growth signaling, *Curr. Opin. Cell Biol. 14*, 104−9.
3. Polesello, C., and Payre, F. (2004) Small is beautiful: what flies tell us about ERM protein function in development, *Trends Cell Biol. 14*, 294−302.
4. Takeuchi, K., Sato, N., Kasahara, H., Funayama, N., Nagafuchi, A., Yonemura, S., Tsukita, S., and Tsukita, S. (1994) Perturbation of cell adhesion and microvilli formation by antisense oligonucleotides to ERM family members, *J. Cell Biol. 125*, 1371−84.
5. Gould, K. L., Bretscher, A., Esch, F. S., and Hunter, T. (1989) cDNA cloning and sequencing of the protein-tyrosine kinase substrate, ezrin, reveals homology to band 4.1, *EMBO J. 8*, 4133−42.
6. Lankes, W. T., and Furthmayr, H. (1991) Moesin: a member of the protein 4.1-talin-ezrin family of proteins, *Proc. Natl. Acad. Sci. U.S.A. 88*, 8297−301.
7. Funayama, N., Nagafuchi, A., Sato, N., Tsukita, S., and Tsukita, S. (1991) Radixin is a novel member of the band 4.1 family, *J. Cell Biol. 115*, 1039−48.
8. Gary, R., and Bretscher, A. (1995) Ezrin self-association involves binding of an N-terminal domain to a normally masked C-terminal domain that includes the F-actin binding site, *Mol. Biol. Cell 6*, 1061−75.
9. Reczek, D., and Bretscher, A. (1998) The carboxyl-terminal region of EBP50 binds to a site in the amino-terminal domain of ezrin that is masked in the dormant molecule, *J. Biol. Chem. 273*, 18452−8.
10. Takahashi, K., Sasaki, T., Mammoto, A., Takaishi, K., Kameyama, T., Tsukita, S., Tsukita, S., and Takai, Y. (1997) Direct interaction of the Rho GDP dissociation inhibitor with ezrin/radixin/moesin initiates the activation of the Rho small G protein, *J. Biol. Chem. 272*, 23371−5.
11. Yonemura, S., Hirao, M., Doi, Y., Takahashi, N., Kondo, T., Tsukita, S., and Tsukita, S. (1998) Ezrin/radixin/moesin (ERM) proteins bind to a positively charged amino acid cluster in the juxta-membrane cytoplasmic domain of CD44, CD43, and ICAM-2, *J. Cell Biol. 140*, 885−95.
12. Heiska, L., Alfthan, K., Gronholm, M., Vilja, P., Vaheri, A., and Carpen, O. (1998) Association of ezrin with intercellular adhesion molecule-1 and -2 (ICAM-1 and ICAM-2). Regulation by phosphatidylinositol 4,5- bisphosphate, *J. Biol. Chem. 273*, 21893−900.
13. Parlato, S., Giammarioli, A. M., Logozzi, M., Lozupone, F., Matarrese, P., Luciani, F., Falchi, M., Malorni, W., and Fais, S. (2000) CD95 (APO-1/Fas) linkage to the actin cytoskeleton through ezrin in human T lymphocytes: a novel regulatory mechanism of the CD95 apoptotic pathway, *EMBO J. 19*, 5123−34.
14. Serrador, J. M., Nieto, M., Alonso-Lebrero, J. L., del Pozo, M. A., Calvo, J., Furthmayr, H., Schwartz-Albiez, R., Lozano, F., Gonzalez-Amaro, R., Sanchez-Mateos, P., and Sanchez-Madrid, F. (1998) CD43 interacts with moesin and ezrin and regulates its redistribution to the uropods of T lymphocytes at the cell−cell contacts, *Blood 91*, 4632−44.

15. Serrador, J. M., Alonso-Lebrero, J. L., del Pozo, M. A., Furthmayr, H., Schwartz-Albiez, R., Calvo, J., Lozano, F., and Sanchez-Madrid, F. (1997) Moesin interacts with the cytoplasmic region of intercellular adhesion molecule-3 and is redistributed to the uropod of T lymphocytes during cell polarization, *J. Cell Biol. 138*, 1409−23.
16. Denker, S. P., Huang, D. C., Orlowski, J., Furthmayr, H., and Barber, D. L. (2000) Direct binding of the Na•••H exchanger NHE1 to ERM proteins regulates the cortical cytoskeleton and cell shape independently of H(+) translocation, *Mol. Cell 6*, 1425−36.
17. Turunen, O., Wahlstrom, T., and Vaheri, A. (1994) Ezrin has a COOH-terminal actin-binding site that is conserved in the ezrin protein family, *J. Cell Biol. 126*, 1445−53.
18. Berryman, M., and Bretscher, A. (2000) Identification of a novel member of the chloride intracellular channel gene family (CLIC5) that associates with the actin cytoskeleton of placental microvilli, *Mol. Biol. Cell 11*, 1509−21.
19. Pestonjamasp, K., Amieva, M. R., Strassel, C. P., Nauseef, W. M., Furthmayr, H., and Luna, E. J. (1995) Moesin, ezrin, and p205 are actin-binding proteins associated with neutrophil plasma membranes, *Mol. Biol. Cell 6*, 247−59.
20. Martin, M., Andreoli, C., Sahuquet, A., Montcourrier, P., Algrain, M., and Mangeat, P. (1995) Ezrin NH2-terminal domain inhibits the cell extension activity of the COOH-terminal domain, *J. Cell Biol. 128*, 1081−93.
21. Henry, M. D., Gonzalez Agosti, C., and Solomon, F. (1995) Molecular dissection of radixin: distinct and interdependent functions of the amino- and carboxy-terminal domains, *J. Cell Biol. 129*, 1007−22.
22. Pearson, M., Reczek, D., Bretscher, A., and Karplus, P. (2000) Structure of the ERM protein moesin reveals the FERM domain fold masked by an extended actin binding tail domain, *Cell 101*, 259−70.
23. Finnerty, C. M., Chambers, D., Ingraffea, J., Faber, H. R., Karplus, P. A., and Bretscher, A. (2004) The EBP50-moesin interaction involves a binding site regulated by direct masking on the FERM domain, *J. Cell Sci. 117*, 1547−52.
24. Smith, W. J., Nassar, N., Bretscher, A., Cerione, R. A., and Karplus, P. A. (2003) Structure of the active N-terminal domain of Ezrin. Conformational and mobility changes identify keystone interactions, *J. Biol. Chem. 278*, 4949−56.
25. Hamada, K., Matsui, T., Tsukita, S., and Hakoshima, T. (2000) Crystallographic characterization of the membrane-binding domain of radixin, *Acta Crystallogr., Sect. D 56*, 922−3.
26. Edwards, S. D., and Keep, N. H. (2001) The 2.7 Å crystal structure of the activated FERM domain of moesin: an analysis of structural changes on activation, *Biochemistry 40*, 7061−8.
27. Nakamura, F., Amieva, M. R., and Furthmayr, H. (1995) Phosphorylation of threonine 558 in the carboxyl-terminal actin-binding domain of moesin by thrombin activation of human platelets, *J. Biol. Chem. 270*, 31377−85.
28. Matsui, T., Maeda, M., Doi, Y., Yonemura, S., Amano, M., Kaibuchi, K., Tsukita, S., and Tsukita, S. (1998) Rho-kinase phosphorylates COOH-terminal threonines of ezrin/radixin/moesin (ERM) proteins and regulates their head-to-tail association, *J. Cell Biol. 140*, 647−57.
29. Nakamura, F., Huang, L., Pestonjamasp, K., Luna, E. J., and Furthmayr, H. (1999) Regulation of F-actin binding to platelet moesin in vitro by both phosphorylation of threonine 558 and polyphosphatidylinositides, *Mol. Biol. Cell 10*, 2669−85.
30. Simons, P. C., Pietromonaco, S. F., Reczek, D., Bretscher, A., and Elias, L. (1998) C-terminal threonine phosphorylation activates ERM proteins to link the cell's cortical lipid bilayer to the cytoskeleton, *Biochem. Biophys. Res. Commun. 253*, 561−5.
31. Fievet, B. T., Gautreau, A., Roy, C., Del Maestro, L., Mangeat, P., Louvard, D., and Arpin, M. (2004) Phosphoinositide binding and phosphorylation act sequentially in the activation mechanism of ezrin, *J. Cell Biol. 164*, 653−9.
32. Oshiro, N., Fukata, Y., and Kaibuchi, K. (1998) Phosphorylation of moesin by rho-associated kinase (Rho-kinase) plays a crucial role in the formation of microvilli-like structures, *J. Biol. Chem. 273*, 34663−6.
33. Gautreau, A., Louvard, D., and Arpin, M. (2000) Morphogenic effects of ezrin require a phosphorylation-induced transition from oligomers to monomers at the plasma membrane, *J. Cell Biol. 150*, 193−203.
34. Gary, R., and Bretscher, A. (1993) Heterotypic and homotypic associations between ezrin and moesin, two putative membrane-cytoskeletal linking proteins, *Proc. Natl. Acad. Sci. U.S.A. 90*, 10846−50.
35. Berryman, M., Gary, R., and Bretscher, A. (1995) Ezrin oligomers are major cytoskeletal components of placental microvilli: a proposal for their involvement in cortical morphogenesis, *J. Cell Biol. 131*, 1231−42.
36. Bretscher, A., Gary, R., and Berryman, M. (1995) Soluble ezrin purified from placenta exists as stable monomers and elongated dimers with masked C-terminal ezrin−radixin−moesin association domains, *Biochemistry 34*, 16830−7.
37. Turunen, O., Sainio, M., Jaaskelainen, J., Carpen, O., and Vaheri, A. (1998) Structure−function relationships in the ezrin family and the effect of tumor-associated point mutations in neurofibromatosis 2 protein, *Biochim. Biophys. Acta 1387*, 1−16.
38. Reczek, D., Berryman, M., and Bretscher, A. (1997) Identification of EBP50: A PDZ-containing phosphoprotein that associates with members of the ezrin−radixin−moesin family, *J. Cell Biol. 139*, 169−79.
39. Laemmli, U. K. (1970) Cleavage of structural proteins during the assembly of the head of bacteriophage T4, *Nature 227*, 680−5.
40. Bretscher, A. (1983) Microfilament organization in the cytoskeleton of the intestinal brush border, *Cell Muscle Motil. 4*, 239−68.
41. Siegel, L. M., and Monty, K. J. (1966) Determination of molecular weights and frictional ratios of proteins in impure systems by use of gel filtration and density gradient centrifugation. Application to crude preparations of sulfite and hydroxylamine reductases, *Biochim. Biophys. Acta 112*, 346−62.
42. Bretscher, A. (1983) Purification of an 80 000 Da protein that is a component of the isolated microvillus cytoskeleton and its localization in nonmuscle cells, *J. Cell Biol. 97*, 425−32.
43. Ishikawa, H., Tamura, A., Matsui, T., Sasaki, H., Hakoshima, T., and Tsukita, S. (2001) Structural conversion between open and closed forms of radixin: low-angle shadowing electron microscopy, *J. Mol. Biol. 310*, 973−8.
44. Hoeflich, K. P., Tsukita, S., Hicks, L., Kay, C. M., and Ikura, M. (2003) Insights into a single rodlike helix in activated radixin required for membrane-cytoskeletal cross-linking, *Biochemistry 42*, 11634−41.
45. Melby, T. E., Ciampaglio, C. N., Briscoe, G., and Erickson, H. P. (1998) The symmetrical structure of structural maintenance of chromosomes (SMC) and MukB proteins: long, antiparallel coiled coils, folded at a flexible hinge, *J. Cell Biol. 142*, 1595−604.
46. Dransfield, D. T., Bradford, A. J., Smith, J., Martin, M., Roy, C., Mangeat, P. H., and Goldenring, J. R. (1997) Ezrin is a cyclic AMP-dependent protein kinase anchoring protein, *EMBO J. 16*, 35−43.
47. Nguyen, R., Reczek, D., and Bretscher, A. (2001) Hierarchy of merlin and ezrin N- and C-terminal domain interactions in homo- and heterotypic associations and their relationship to binding of scaffolding proteins EBP50 and E3KARP, *J. Biol. Chem. 276*, 7621−9.

BI0480382